Toxicology Research

PAPER

View Article Online
View Journal | View Issue

Cite this: *Toxicol. Res.*, 2018, **7**, 931

Bioactive nano-metal–organic frameworks as antimicrobials against Gram-positive and Gram-negative bacteria†

Neha Bhardwaj,‡[a,b] Satish K. Pandey,‡[a] Jyotsana Mehta,[a,b] Sanjeev K. Bhardwaj,[a,b] Ki-Hyun Kim*[c] and Akash Deep*[a,b]

Received 23rd March 2018,
Accepted 10th May 2018

DOI: 10.1039/c8tx00087e

rsc.li/toxicology-research

More effective antibiotics are needed to overcome the problem of multidrug resistance. The antibacterial efficacies of three Zn-based nano metal–organic frameworks (nMOFs) – IRMOF-3, MOF-5, and Zn-BTC – were explored, both alone and as mixtures with ampicillin and kanamycin. When tested against *Escherichia coli*, *Staphylococcus aureus*, *Staphylococcus lentus*, and *Listeria monocytogenes*, the nMOF/drug mixtures demonstrated synergistic (IRMOF-3/kanamycin) or additive (other nMOF/drug combinations) effects compared with the nMOFs or antibiotics alone. Zn-Based nMOFs can reduce the burden of the new discovery of antimicrobial pharmaceuticals by increasing the potency of existing antibiotics.

Introduction

Bacterial infections are a global public health concern and pose a strong economic burden on the healthcare of a nation. Most human infections are caused by Gram-negative (such as *Escherichia coli*, *Pseudomonas aeruginosa*) and Gram-positive (*Staphylococcus aureus*, beta-hemolytic Streptococcus) bacteria.[1–5] The increasing incidences of drug resistance (or multi-drug resistance) of bacterial infections have become serious healthcare challenges.[6,7] However control of bacterial contamination is probably one of the most relevant strategies to minimize the disease outbreaks. In this context, nanomaterials and nanocomposites have emerged as potential antimicrobial agents.[8–16]

Metal organic frameworks (MOFs) are a versatile class of crystalline hybrid materials suitable for a wide range of applications as adsorbents, molecular sieves, photocatalysts, sensors, immobilization substrates, *etc*.[17–24] Biological applications of metal–organic frameworks (MOFs) have been reported in the fields of drug delivery/therapy, biosensing, cosmetics, and enzyme encapsulation.[21,25–31] Because of their large pore size, which allows storage of guest molecules, and their ability to release metal ions, MOFs are attractive antimicrobial materials.[32,33] Other porous materials such as zeolites, activated carbon, and mesoporous silica have been explored for storage and release of antibacterial agents. However, MOFs are advantageous due to their ordered structures, biocompatibility, larger pore size (relative to zeolites), and inherent bactericidal nature due to their metal ions.[32] Recently, MOFs have been investigated for use in storage and multi-rate delivery of antimicrobial agents including small gas molecules such as carbon monoxide, hydrogen sulfide, and nitrogen monoxide, pharmaceuticals such as penicillin, cephalosporin, aminoglycosides, glycopeptides, and macrolides, and metal ions.[34,35] As such to interestingly, for the antimicrobial activity of MOFs is generally attributed to the presence of metallic ions, *e.g.*, Cu, Ca, Fe, Zn, and Ag.[33,36–38] For instance, Ag based MOFs have been reported with antibacterial activity against various groups of bacteria, *e.g.*, *Staphylococcus aureus*, *Escherichia coli and Pseudomonas aeruginosa*.[39,40] The antimicrobial activity of a Cu-BTC MOF immobilized cellulosic fiber has been documented against *Escherichia coli*.[41] The cellulose-MOF system was able to eliminate the growth of *E. coli* on agar plates and liquid cultures. Similarly, a Cu-BTC MOF (coated on silk fibers) has also been reported for its antibacterial activity.[42] The leaching of Cu ions from the MOF contributed toward its antimicrobial activity. A similar mechanism was also attributed to explain the high and long lasting antimicrobial properties of a Co imidazolate MOF.[43,44]

[a]*Central Scientific Instruments Organisation (CSIR-CSIO), Sector 30 C, Chandigarh, 160030, India. E-mail: dr.akashdeep@csio.res.in; Tel: +91-172-2672236*
[b]*Academy of Scientific and Innovative Research, CSIR-CSIO, Sector 30 C, Chandigarh, 160030, India*
[c]*Department of Civil & Environmental Engineering, Hanyang University, 222 Wangsimni-Ro, Seoul 133-791, Republic of Korea. E-mail: kkim61@hanyang.ac.krc; Fax: +82-222201945; Tel: +82-22202325*

† Electronic supplementary information (ESI) available: UV-Vis and FTIR spectroscopic analysis of Zn-nMOF formulations; FE-SEM and XRD analysis of Zn-nMOF formulations; DLS based particle size analysis of nMOF and nMOF/drug combination, and the cytotoxicity of nMOFs alone and combined with antibiotics on HaCaT cells. See DOI: 10.1039/c8tx00087e

‡ Both authors contributed equally.

Zinc-based nanomaterials have been widely utilized in many skin care products (*e.g.*, sunscreen lotions, moisturizers, antidandruff products, and astringents) in light of their enhanced antimicrobial/antibacterial properties.[45,46] However, toxicity analysis of Zn ions has revealed their concentration dependency on neuronal cells. For instance, they were suspected to be cytotoxic to human cells in concentrations exceeding 6.5 μg ml^{-1}.[47] In another study, ZnO nanoparticles were found to induce significant oxidative stress-related cytotoxicity and genotoxicity in human lung fibroblasts (*in vitro*).[48] The concerns about the toxicity of ZnO nanoparticles were also raised as they were found to be highly toxic to NIH/3T3 cells, inducing viability loss, membrane leakage, and morphology changes.[49]

It has been articulated that the cytotoxicity of ZnO nanoparticles can be tailored through diverse routes of modification (*e.g.*, their surface-bound chemical groups, surface charge density, and catalytic activity).[50] In some studies, it has been found out that MOF nanoparticles exhibit low cytotoxicity, comparable to those of other commercialized nanoparticulate systems.[51] Zn-based MOFs have been applied as drug delivery or antibacterial agents owing to their low cytotoxicity profiles.[52–54] Recently, Tabar *et al.* have proposed the use of a Zn based MOF (Zn azelate) as a drug release carrier product with antibacterial activities.[54]

Here, we investigate the antimicrobial activities of several Zn-based nano MOFs, alone and in combination with antibiotics, against Gram-positive (*Staphylococcus aureus*, *Staphylococcus lentus* and *Listeria monocytogenes*) and Gram-negative (*Escherichia coli*) bacteria. We demonstrate that these novel nMOF/drug formulations have synergistic or additive antibacterial effects relative to the nMOFs and drugs alone.

Experimental

Materials

Zinc nitrate hexahydrate [$Zn(NO_3)_2{\cdot}6H_2O$], zinc acetate dihydrate [$Zn(CH_3COO)_2{\cdot}2H_2O$], terephthalic acid (benzenedicarboxylic acid, BDC), amino terephthalic acid (NH_2-BDC), trimesic acid (H_3BTC), triethylamine (TEA), dimethyl sulfoxide (DMSO), dimethylformamide (DMF), and ethanol were purchased from Sigma Aldrich, India. Mueller–Hinton (MH) broth, soybean casein digest medium (tryptone soya broth), and agar were purchased from HIMEDIA, India. All chemicals were used as purchased without further purification. Bacterial strains were procured from the CSIR Institute of Microbial Technology, Chandigarh, India. Bacterial strains were cultured in MH broth and stored at −20 °C with 20% glycerol as frozen stocks. Prior to each experiment, microbial cells were freshly revived from stock on agar plates.

Equipment

UV-Vis spectroscopy (Varian, Cary 5000, Agilent), FTIR spectroscopy (Nicolet iS10, Thermo Fisher), FE-SEM (Hitachi S4300), particle size analysis (Model Nano-ZS90 from Malvern Instruments), and X-ray diffraction (Bruker X8 Advance) were used to characterize synthesized MOFs.

Synthesis of nano MOFs

Three Zn-based nMOFs – IRMOF-3, MOF-5, and Zn-BTC – were synthesized as previously described.[55–57]

Synthesis of IRMOF-3

IRMOF-3 was synthesized using the fast precipitation method. Briefly, 2.4 g of $Zn(NO_3)_2{\cdot}6H_2O$ and 0.66 g of NH_2-BDC were added into 80 mL of dimethylformamide (DMF) and mixed by stirring. Thereafter, 500 μL of triethylamine (TEA) was added dropwise, leading to the immediate formation of white precipitates. The contents were stirred for 2 h, followed by collection of the product by centrifugation at 10 000 rpm for 15 min. The resulting white IRMOF-3 powder was washed three times with DMF and then left in contact with chloroform for 3 days; the solvent was substituted with a fresh supply every 24 h. Finally, the nMOF was obtained by filtering the solution and drying under vacuum at 70 °C. All powdered synthesized nMOF samples were stored in dry containers under room temperature conditions (RT, 25 ± 2 °C) and used as such for determining their antibacterial activity.

Synthesis of MOF-5

Under vigorous stirring, 1.2 g of $Zn(NO_3)_2{\cdot}6H_2O$ and 0.334 g of BDC were mixed with 40 mL of DMF. The reaction contents were then placed in an ultrasonic bath followed by dropwise addition of 2.2 mL of TEA. After a 45 min reaction, a solid white product was recovered by centrifugation (15 000 rpm, 30 min). The MOF-5 product was then washed three times with DMF, dried at 100 °C for 5 h, and stored in sealed vials.

Synthesis of Zn-BTC

For the synthesis of Zn-BTC, 1.05 g of 0.5 M H_3BTC was dissolved in 20 mL of 20% ethanol. In a separate preparation, 1.81 g of zinc acetate dihydrate ($Zn(CH_3COO)_2{\cdot}2H_2O$) was dissolved in 50 mL of 20% ethanol solution. The above two solutions were mixed and ultrasonicated for 45 min. The precipitate formed by the above reaction was filtered followed by washing with water and ethanol in that order. The final product was dried at 70 °C.

Incorporation of drugs with MOFs

In each case, a 25 mg dried sample of nMOF (IRMOF-3, MOF-5, or Zn-BTC) was weighed and mixed with 5 mL of 1 mg mL^{-1} suspension of ampicillin or kanamycin (in 20% acetonitrile). After sealing the ampule tightly, the mixture was left for stirring for 24 hours (at 100 rpm) under room temperature conditions. Next, the supernatant was separated after centrifugation (5000 rpm; 20 min) and the obtained drug loaded nMOF sample was immediately washed with 10 mL of 10 mM phosphate buffer saline (PBS). A subsequent centrifugation was performed to remove any surface adsorbed drug content. The prepared sample was then allowed to dry overnight at 50 °C in an oven.

Antibacterial activity

The MIC values of the Zn-nMOFs against the four bacterial species were evaluated using the standard broth microdilution method recommended by the Clinical and Laboratory Standards Institute.[58] Bacteria were grown overnight and diluted in MH broth to attain a cell density of 10^7 colony forming units (CFU) per mL in a 96-well flat-bottomed microtiter plate. Then, 100 μL of the dispersed sample of nMOF or nMOF/antibiotic mix (concentrations in the range of 1–1000 μg mL^{-1}) was introduced into the microtiter plates. Ampicillin and kanamycin were used as positive controls. Several experiments of a particular batch study were executed simultaneously in the microtiter plate. The microtiter plate was incubated at 37 °C for 24 h followed by measurement of the optical density at 600 nm using a microplate reader.

Fractional inhibitory concentrations (FICs)

Checkerboard microtiter tests were performed to determine FIC values and FIC indices to assess whether the nMOFs and antibiotics demonstrated a synergistic, additive, or indifferent effect when used as a mixture. The experimental procedures were based on the protocols described by Elion and co-workers.[59] In brief, different serial dilutions of individual nMOFs and antibiotics as well as their mixtures were prepared. The concentrations were maintained to ensure a dose of 0.016-2X of the MIC of nMOF or antibiotic. A 20 μL aliquot of the sample was introduced into the wells of a 96-well plate in a vertical orientation, while the same volume of each antibiotic dilution was introduced in a horizontal orientation. Thus, a single microtiter plate was used for the study of different combinations of the above agents. Next, 160 μL (10^7 CFU mL^{-1}) of bacterial solution (*S. aureus*, *S. lentus*, *E. coli*, and *L. monocytogenes*) were introduced, and the plate was incubated at 37 °C for 24 h. Blank wells (without any antibacterial agent) were used as positive controls. FIC values for different nMOFs ($FIC_{IRMOF\text{-}3}$, $FIC_{Zn\text{-}BTC}$, $FIC_{MOF\text{-}5}$) and antibiotics (FIC_{Amp}, FIC_{Kan}) were calculated according to the following equation.[60]

$$FIC_{nMOF/antibiotic} = MIC_{nMOF+antibiotic}/MIC_{nMOF/antibiotic} \quad (1)$$

The FIC index, obtained as $FIC_{nMOF} + FIC_{antibiotic}$, was used to interpret the nature of the cumulative antimicrobial effect when the nMOF and antibiotic were used as a mixture. The FIC index values ≤0.5, 0.5–1.0, 1.0–4.0, and ≥4.0 were used to describe the system as synergistic, additive, indifferent, and antagonistic, respectively.

Time-kill assays

The kinetics of bactericidal activity was studied for nMOFs alone and nMOF/antibiotic mixtures. For this comparative analysis, samples at their MIC concentrations were introduced into 20 mL of MH broth containing 10^7 CFU mL^{-1} of *S. aureus*, *S. lentus*, *E. coli*, or *L. monocytogenes*. The contents were stirred at 200 rpm and incubated at 37 °C. During the test, a 100 μL culture sample was periodically collected at different time intervals (0, 4, 8, 12, 16, 20, and 24 h). This sample was plated on MH agar plates and incubated at 37 °C for 24 h followed by counting of colony forming units.

Cytotoxicity analysis

Human cell toxicity of the nMOFs and nMOF/antibiotic mixtures was assessed using HaCaT cells and an MTT assay (MTT is 3-(4,5-dimethylthiazol-2-yl)-2,5-diphenyltetrazolium bromide).[61–63] Briefly, HaCaT cells (9×10^4 per well) were seeded in triplicate in a 96-well plate containing RPMI-1640 supplemented with 5% fetal bovine serum. The temperature (37 °C) and humidified CO_2 (5%) conditions were maintained overnight in an incubator. The next day, nMOFs and nMOF/antibiotic samples were added in distinct wells at their MIC values. The plate was again incubated for 24 h at 37 °C. Thereafter, the cells were treated with 20 μL of MTT solution (2.5 mg mL^{-1} in PBS) and incubated for 4 h at 37 °C. The supernatant was separated, and the resulting formazan crystals were dissolved in 100 μL of dimethyl sulfoxide (DMSO). The samples were measured for absorbance at 570 nm with a microplate reader. The comparative viability of cells was calculated by the OD_{570} ratio between the treated and untreated cells.

Results and discussion

Structural and morphological characterization

The UV-Vis absorbance (200–800 nm) and FTIR spectra of IRMOF-3, Zn-BTC, and MOF-5 are shown in Fig. S1.† IRMOF-3 shows a characteristic excitation peak at 340 nm due to the charge transfer mechanism from ligand-to-metal (Fig. S1A†).[64] The FTIR spectrum of IRMOF-3 (Fig. S1B†) shows bands around 1600–1330 cm^{-1} signifying the asymmetric and symmetric carboxyl group vibrations. The bands from 3100–3500 cm^{-1} correspond to the amine groups present in IRMOF-3.[65,66] The UV-Vis spectrum of MOF-5 shows a broad absorbance peak near 240 nm, which is characteristic of the organic ligand (Fig. S1C†).[67] The FTIR spectrum of MOF-5 (Fig. S1D†) shows bands between 1500–1600 cm^{-1} and 1330–1400 cm^{-1} attributed to the –COO asymmetric stretching vibration and –COO symmetric stretching vibration, respectively. The multiple weak bands between 1000–1150 cm^{-1} and 650–850 cm^{-1} represent the ring-in and out-of-plane bending vibration of aromatic C–H bonds, respectively.[68] The bands at 1665 and 1599 cm^{-1} are assigned to the C=O bond stretching vibration and aromatic C–C bond vibration of the organic linker BDC, respectively. A sharp band centered at 1385 cm^{-1} is attributed to the C–O bond stretching vibration. The sample of the synthesized Zn-BTC showed a characteristic absorption peak at 250 nm along with a smaller peak at ~290 nm (Fig. S1E†). These peaks signified the successful incorporation of the organic linker BTC in the MOF.[69] The FTIR spectrum of Zn-BTC showed bands for the symmetric and asymmetric vibration of BTC at 1479–1374 cm^{-1} and 1564–1532 cm^{-1}, respectively (Fig. S1F†). The broad bands around 3460 and

3125 cm^{-1} along with a sharp band near 1620 cm^{-1} are representative of water molecules entrapped within the metal coordination spheres. The absence of a carboxylic group absorption band at 1730–1700 cm^{-1} indicates that the organic linker (BTC) is bonded with the metal center, probably in a monodentate form.[70]

Structural analysis of the synthesized Zn-nMOFs was performed using XRD and FE-SEM (Fig. S2†). XRD and FE-SEM imaging (Fig. S2A and S2B†) revealed the crystallinity of IRMOF-3.[55] The synthesized crystals were rectangular cuboids with a homogenous product formation. The surface morphology of MOF-5 indicated that the particle size ranged from 5–10 μm (Fig. S2C†). The XRD pattern (Fig. S2D†) showed reflection peaks at 9.7°, 13.7°, 15.3°, 17.8°, 19.5°, 20.6°, 24.6°, 26.5°, 30°, 31.6°, 34.6°, 36.2°, and 42.6°, correlating well with a previous study.[71] The XRD and FE-SEM data for Zn-BTC (Fig. S2E and S2F†) agree with previous reports.[72,73] The product possessed a rod-like morphology.

The particle size analysis of nMOFs was made to assess the changes between before and after the loading of drugs using the dynamic light scattering technique. As shown in Fig. S3,† the average hydrodynamic particle size of the nMOF (MOF-5, shown as a representative MOF) did not change after its mixing with the drug (ampicillin). These studies suggest that the drug molecules were absorbed within the pores of the nMOF (*e.g.*, without conjugation on the surface). All other examples of nMOFs and drug combinations were also characterized with similar observation.

Antibacterial activity

Table 1 summarizes the antimicrobial activity (minimal inhibitory concentrations (MICs)) of the three Zn-nMOFs and two antibiotics (ampicillin and kanamycin) individually and when used as mixtures, against the four microorganisms *S. aureus, S. lentus*, *E. coli*, and *L. monocytogenes*. All six nMOF/drug mixtures showed significant antimicrobial activity against all four microorganisms. Notably, nMOF/drug mixtures showed greater antibacterial activity than the nMOF or drug alone, indicated by lower MIC values for both the antibiotic and (in most cases) the nMOF.[58] For example, MIC values for the three Zn-nMOFs, Zn-BTC, IRMOF-3, and MOF-5, and ampicillin when used individually against *S. aureus* were 200, 100, 200, and 32 μg mL^{-1}, respectively (Table 1A). When used as nMOF/ampicillin mixtures, the MIC values were reduced to 150 μg mL^{-1} for both Zn-BTC and MOF-5 (the MIC for IRMOF-3 remained unchanged), and the MIC value for ampicillin was reduced 2-fold to 16 μg mL^{-1} in each case (Table 1B). MIC values for ampicillin against the four microorganisms were reduced 2-fold to 4-fold when combined with a Zn-MOF; MIC values for kanamycin were reduced 1.5-fold to as much as 8-fold (against *E. coli* when combined with IRMOF-3). These results indicate that the Zn-nMOF/drug combinations had synergistic or additive antibacterial effects against both Gram-positive and Gram-negative bacteria. IRMOF-3/ampicillin was the most potent combination against the three Gram-positive bacteria; for Gram-negative *E. coli*, all three nMOF/drug combi-

Table 1 Minimum inhibitory concentrations (MICs) of nMOFs and drugs when used individually and as mixtures against various bacterial strains

A. MICs of nMOFs and drugs when used individually

			MIC (μg mL^{-1})			
Order	Class	nMOF drug	*S. aureus*	*S. lentus*	*L. monocytogenes*	*E. coli*
1	MOF	Zn-BTC	200	200	250	150
2		IRMOF-3	100	150	150	100
3		MOF-5	200	200	200	200
4	Antibiotic	Ampicillin	32	48	48	32
5		Kanamycin	32	32	24	32

B. MICs of nMOFs and drugs when used as a mixture

			MIC (μg mL^{-1})			
Order	Class	nMOF/drug	*S. aureus*	*S. lentus*	*L. monocytogenes*	*E. coli*
1	nMOF + ampicillin	Zn-BTC	150	150	100	100
2		Ampicillin	16	24	16	8
3		IRMOF-3	100	50	50	50
4		Ampicillin	16	16	16	8
5		MOF-5	100	150	100	100
6		Ampicillin	16	24	24	8
7	nMOF + kanamycin	Zn-BTC	100	100	100	100
8		Kanamycin	16	16	16	16
9		IRMOF-3	50	50	100	25
10		Kanamycin	8	8	8	4
11		MOF-5	100	100	100	100
12		Kanamycin	8	8	16	8

nations displayed a similar higher bactericidal activity than the nMOFs or drugs alone.

The metal–organic framework structure behaves as a reservoir for Zn^{+2} ions that interact with the bacterial cell wall. A high loading of Zn^{+2} ions increases the antibacterial potency of the compounds.[54,72,74] Although the Zn-nMOFs alone did not show exceptional antibacterial activity (MIC values ranged from 100–250 μg mL^{-1}), when mixed with ampicillin or kanamycin, the resulting formulations surpassed the antibacterial efficiency of these drugs alone against both Gram-positive and Gram-negative bacteria.

The mechanism of antimicrobial action of the nMOF/drug combination is depicted in Fig. 1. As such, a system can facilitate antimicrobial action *via* inhibition or regulation of enzymes involved in cell wall biosynthesis, nucleic acid metabolism, repair, protein synthesis, and disruption of the membrane structure. The antimicrobial action of MOFs is generally associated with physical damage to bacterial cells. The MOFs can act as a reservoir of metal ions, which are gradually released to result in a sustained antibacterial action analogous to that of other well-known metal/metal oxide nanoparticles. In our case, the plasma membrane disorganization was also evident from the FE-SEM studies of some representative samples, *i.e.*, IRMOF-3/ampicillin and IRMOF-3/kanamycin treated *E. coli* and *S. aureus* cells (Fig. 2). As shown in this representative study, 4 hours of incubation of IRMOF-3/ampicillin and IRMOF-3/kanamycin with *E. coli* and *S. aureus* resulted in cell disruption.

Fractional inhibitory concentrations (FICs)

To assess whether the nMOF/drug combinations showed synergistic, additive, or indifferent effects, we used checkerboard microtiter tests to determine the fractional inhibitory concentrations (FICs) of the nMOFs and drugs when used individually and in combination against the four bacterial species and FIC indices for the nMOF/drug combinations (Table 2).[59,60] A synergistic interaction was observed for IRMOF-3/kanamycin against *E. coli*, as indicated by an FIC index ≤0.5. All other IRMOF-3/drug combinations showed additive effects (FIC index between 0.5 and 1) except for IRMOF-3/ampicillin against *S. aureus* (FIC index = 1.5, indicating an indifferent interaction). An additive interaction was observed for MOF-5/kanamycin against all four microorganisms (FIC index = 0.75 in each case) and for MOF-5/ampicillin against *E. coli*. Additive interactions were observed for Zn-BTC/ampicillin against *L. monocytogenes* and *E. coli* and for Zn-BTC/kanamycin against *L. monocytogenes*. Other MOF-5/drug and Zn-BTC/drug combinations showed indifferent interactions against the microorganisms, with FIC indices ranging from 1 to 1.25.

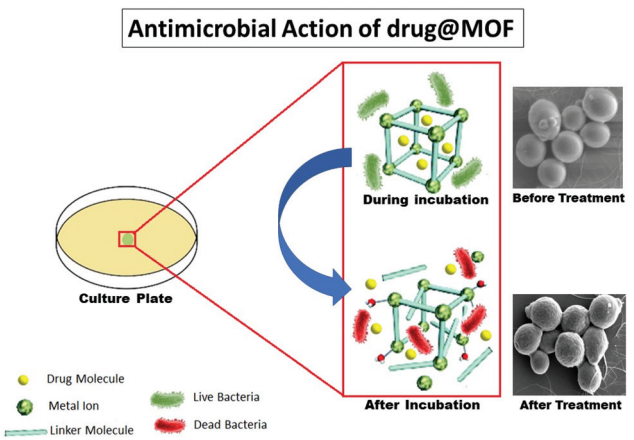

Fig. 1 Mechanism of antimicrobial action of nMOF/drug mixtures.

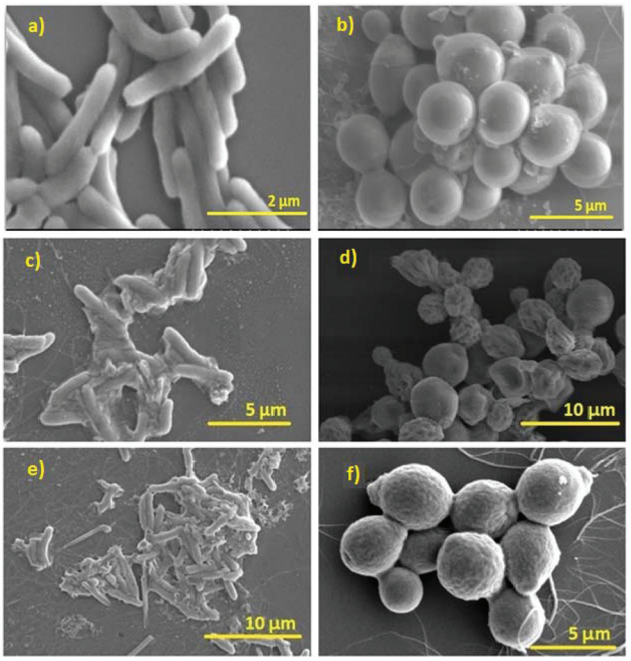

Fig. 2 FE-SEM images of diverse samples for toxicity studies: (a) untreated *E. coli*; (b) untreated *S. aureus*; (c) IRMOF-3/ampicillin treated *E. coli*; (d) IRMOF-3/ampicillin treated *S. aureus*; (e) IRMOF-3/kanamycin treated *E. coli*; and (f) IRMOF-3/kanamycin treated *S. aureus*.

Time-kill assays and cytotoxicity analysis

All nMOF/drug combinations showed bactericidal effects. The kinetics of these effects was measured using time-kill assays, with drugs used at their minimum inhibitory concentrations (Fig. 3 and 4 for nMOF/ampicillin and nMOF/kanamycin combinations, respectively). In general, nMOF/drug combinations showed similar or slightly slower bactericidal effects over 24 h than the drug alone, while using lower drug combinations (due to the lower MIC values for the drugs when used in a nMOF/drug mixture). For example, against *E. coli*, IRMOF-3/ampicillin and MOF-5/ampicillin showed similar bactericidal kinetics to ampicillin alone, while Zn-BTC/ampicillin showed slower kinetics and a higher bacterial count after 24 h (Fig. 3a). Zn-BTC/ampicillin against *E. coli* showed the weakest bactericidal effect of all MOF/drug/microorganism combi-

Table 2 Fractional inhibitory concentrations (FICs) and FIC indices

A. FICs of nMOFs and drugs when used individually

			FIC			
Order	Class	nMOF/drug	*S. aureus*	*S. lentus*	*L. monocytogenes*	*E. coli*
1	nMOF + ampicillin	Zn-BTC	0.75	0.75	0.4	0.66
2		Ampicillin	0.5	0.5	0.33	0.25
3		IRMOF-3	1	0.33	0.33	0.5
4		Ampicillin	0.5	0.33	0.33	0.25
5		MOF-5	0.5	0.75	0.5	0.5
6		Ampicillin	0.5	0.5	0.5	0.25
7	nMOF + kanamycin	Zn-BTC	0.5	0.5	0.4	0.66
8		Kanamycin	0.5	0.5	0.5	0.5
9		IRMOF-3	0.5	0.66	0.66	0.25
10		Kanamycin	0.25	0.25	0.25	0.25
11		MOF-5	0.5	0.5	0.5	0.5
12		Kanamycin	0.25	0.25	0.25	0.25

B. FIC indices of nMOF/drug mixtures

			FIC Index			
Order	MOF	Drug	*S. aureus*	*S. lentus*	*L. monocytogenes*	*E. coli*
1	Zn-BTC	Ampicillin	1.25	1.25	0.73	0.91
2		Kanamycin	1	1	0.9	1.16
3	IRMOF-3	Ampicillin	1.5	0.66	0.66	0.75
4		Kanamycin	0.75	0.91	0.91	0.5
5	MOF-5	Ampicillin	1	1	1	0.75
6		Kanamycin	0.75	0.75	0.75	0.75

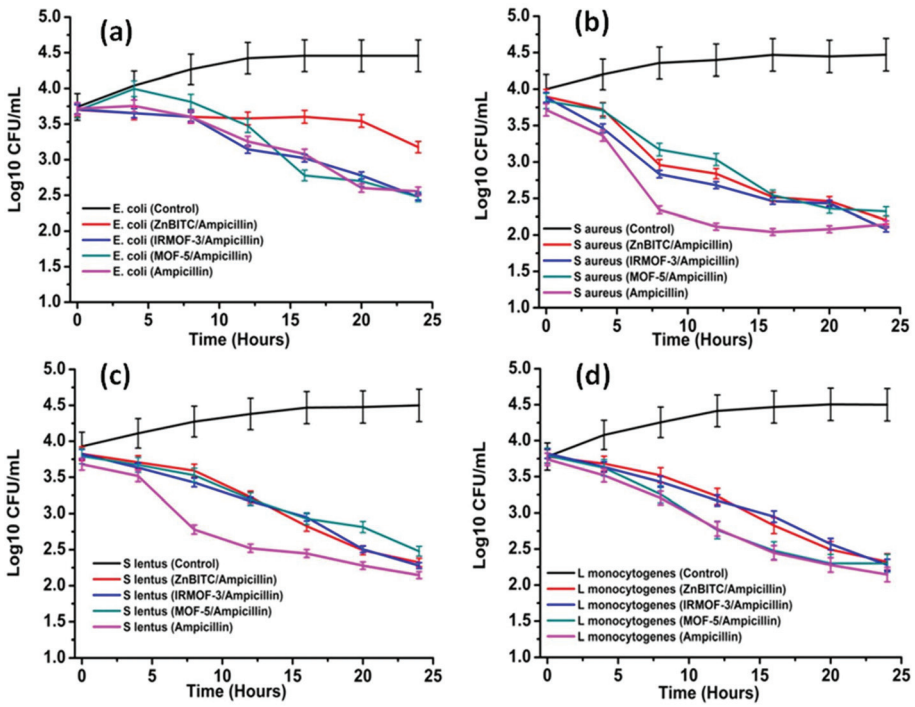

Fig. 3 Time-kill assay results for nMOF/ampicillin mixtures against: (a) *E. coli*, (b) *S. aureus*, (c) *S. lentus*, and (d) *L. monocytogenes*. Data points represent mean values from triplicate analysis. Values are represented as means ± S.D of three independent values.

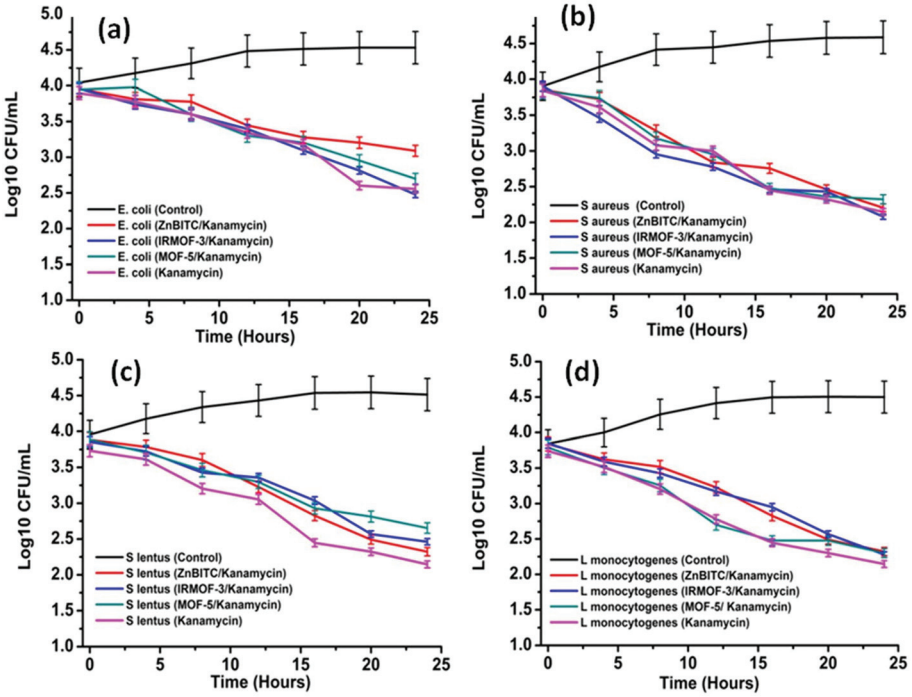

Fig. 4 Time-kill assay results for nMOF/kanamycin mixtures against: (a) *E. coli*, (b) *S. aureus*, (c) *S. lentus*, and (d) *L. monocytogenes*. Values are represented as means ± S.D of three independent values.

nations. All other nMOF/ampicillin combinations reduced bacterial colonies by 1 to 1.5 log units over 24 h (Fig. 3). All nMOF/kanamycin combinations reduced bacterial colonies by 0.75 to 2 log units over 24 h (Fig. 4).

In the literature, other MOF/antibiotic combinations have also been reported as antibacterials, including MOF-53/vancomycin, HKUST-1/metronidazole, and Ni-CPO-27/metronidazole.[34,53,75] Nanomaterials such as silver nanoparticles (AgNPs) capped with peptides and combined with antibiotics have also been tested. These formulations have shown increased bactericidal activity, allowing 2- to 10-fold lower dosage of antibiotic for an equivalent bactericidal effect.[76,77] These previous studies also suggest that nMOF/antibiotic combination therapy might be superior to that of monotherapy, with the advantage of a reduced dose requirement.[78–80]

In some separate experiments, we have also tested some other nMOFs – NH_2-MIL-53(Fe), MIL-53(Al), and NH_2-UiO-66 (Zr) – in combination with antibiotics; however, no significant additional antimicrobial activity was observed (data not shown).

To assess human cell viability during nMOF/drug application, we tested the effects of the Zn-nMOF/drug combinations on human dermal noncancerous (HaCaT) cells (Fig. S4†). All nMOFs and drugs were tested at their MIC concentrations. The results indicated low toxicity (10–25%) for Zn-BTC with both drugs and MOF-5/ampicillin while moderate toxicity (30–45%) was observed for IRMOF-3 with both drugs and MOF-5/kanamycin.

Statistical analysis

All Zn-nMOF/antibiotic formulations showed significantly higher antibacterial activities than the antibiotic alone. In all cases, the *P*-value was ≤0.05, indicating a significant difference in the antibacterial efficacy of the mixture *versus* the antibiotic alone based on MIC measurements. For IRMOF-3, MOF-5, and Zn-BTC combined with ampicillin against *S. aureus*, the results of one-way ANOVA gave *P*-values of 0.002, 0.03, and 0.05, respectively; against *S. lentus*, the *P*-values were 0.032, 0.01, and 0.01, respectively; against *L. monocytogenes*, the *P*-values were 0.032, 0.01 and 0.01, respectively; and against *E. coli*, the *P*-values were 0.03, 0.04, and 0.035, respectively. *P*-Values were ≤0.05 for the three Zn-MOFs combined with kanamycin for all four tested bacteria.

Conclusions

In conclusion, this study demonstrates that Zn-nMOF/antibiotic formulations have significantly improved antibacterial activity compared to antibiotics alone. Zn-nMOFs offer a new approach to combat MDR bacterial strains and reduce the burden of new drug discoveries. This study paves the way for the development of new porous nMOFs for biological and medical applications. Combination therapy using nMOFs and antibiotics can be used to increase the antimicrobial activity and broaden the antimicrobial spectrum.

Author contributions

N.B. and S.K.P contributed equally. They designed and carried out MOF synthesis and characterization, antimicrobial activity tests, time-kill assays, FIC calculations, and cell viability tests. J.M. assisted with the characterization of nanomaterials. S.B. performed antimicrobial activity tests and helped in data analysis. K.H.-K. contributed to the interpretation of results and wrote the manuscript. A.D. supervised the work, contributed to the experimental design, interpretation of results and preparation of the manuscript.

Conflicts of interest

The authors have declared that no conflicting interest exists.

Acknowledgements

The research was funded by the DBT (Department of Biotechnology), India project (No. BT/PR18868/BCE/8/1370/2016). S. K. P, S. K. B. and J. M. thank DST, CSIR-SRF and UGC, New Delhi, India, respectively for their research fellowships. The authors thank the Director of CSIR-CSIO, Chandigarh, India, for providing infrastructural facilities. K. H. K. acknowledges the support from grants from the National Research Foundation of Korea (NRF) funded by the Ministry of Science, ICT, & Future Planning (No. 2016R1E1A1A01940995).

References

1 S. M. Opal and J. Cohen, Clinical gram-positive sepsis: does it fundamentally differ from gram-negative bacterial sepsis?, *Crit. Care Med.*, 1999, **27**, 1608–1616.
2 N. Sylvetsky, D. Raveh, Y. Schlesinger, B. Rudensky and A. M. Yinnon, Bacteremia due to beta-hemolytic Streptococcus group G: increasing incidence and clinical characteristics of patients, *Am. J. Med.*, 2002, **112**, 622–626.
3 M. A. Croxen, R. J. Law, R. Scholz, K. M. Keeney, M. Wlodarska and B. B. Finlay, Recent advances in understanding enteric pathogenic *Escherichia coli*, *Clin. Microbiol. Rev.*, 2013, **26**, 822–880.
4 F. L. Short, S. L. Murdoch and R. P. Ryan, Polybacterial human disease: the ills of social networking, *Trends Microbiol.*, 2014, **22**, 508–516.
5 S. Jarraud, C. Mougel, J. Thioulouse, G. Lina, H. Meugnier, F. Forey, X. Nesme, J. Etienne and F. Vandenesch, Relationships between Staphylococcus aureus genetic background, virulence factors, agr groups (alleles), and human disease, *Infect. Immun.*, 2002, **70**, 631–641.
6 S. B. Levy, Multidrug resistance—a sign of the times, *N. Engl. J. Med.*, 1998, **338**, 1376–1378.
7 J. P. Burnham, M. A. Lane and M. H. Kollef, Impact of sepsis classification and multidrug resistance status on outcome among patients treated with appropriate therapy, *Crit. Care Med.*, 2015, **43**, 1580.
8 B. D. Brooks and A. E. Brooks, Therapeutic strategies to combat antibiotic resistance, *Adv. Drug Delivery Rev.*, 2014, **78**, 14–27.
9 R. Laxminarayan, A. Duse, C. Wattal, A. K. Zaidi, H. F. Wertheim, N. Sumpradit, E. Vlieghe, G. L. Hara, I. M. Gould and H. Goossens, Antibiotic resistance—the need for global solutions, *Lancet Infect. Dis.*, 2013, **13**, 1057–1098.
10 E. E. Gill, O. L. Franco and R. Hancock, Antibiotic adjuvants: diverse strategies for controlling drug-resistant pathogens, *Chem. Biol. Drug Des.*, 2015, **85**, 56–78.
11 J. D. Siegel, E. Rhinehart, M. Jackson and L. Chiarello, Management of multidrug-resistant organisms in health care settings, 2006, *Am. J. Infect. Control*, 2007, **35**, S165–S193.
12 D. A. Goldmann, R. A. Weinstein, R. P. Wenzel, O. C. Tablan, R. J. Duma, R. P. Gaynes, J. Schlosser, W. J. Martone, J. Acar and J. Avorn, Strategies to prevent and control the emergence and spread of antimicrobial-resistant microorganisms in hospitals: a challenge to hospital leadership, *J. Am. Med. Assoc.*, 1996, **275**, 234–240.
13 R. Loddenkemper, D. Sagebiel and A. Brendel, Strategies against multidrug-resistant tuberculosis, *Eur. Respir. J.*, 2002, **20**, 66s–77s.
14 A. J. Huh and Y. J. Kwon, "Nanoantibiotics": a new paradigm for treating infectious diseases using nanomaterials in the antibiotics resistant era, *J. Controlled Release*, 2011, **156**, 128–145.
15 L. S. Jabr-Milane, L. E. van Vlerken, S. Yadav and M. M. Amiji, Multi-functional nanocarriers to overcome tumor drug resistance, *Cancer Treat. Rev.*, 2008, **34**, 592–602.
16 C. E. Soma, C. Dubernet, D. Bentolila, S. Benita and P. Couvreur, Reversion of multidrug resistance by co-encapsulation of doxorubicin and cyclosporin A in polyalkylcyanoacrylate nanoparticles, *Biomaterials*, 2000, **21**, 1–7.
17 S. L. James, Metal-organic frameworks, *Chem. Soc. Rev.*, 2003, **32**, 276–288.
18 R. J. Kuppler, D. J. Timmons, Q.-R. Fang, J.-R. Li, T. A. Makal, M. D. Young, D. Yuan, D. Zhao, W. Zhuang and H.-C. Zhou, Potential applications of metal-organic frameworks, *Coord. Chem. Rev.*, 2009, **253**, 3042–3066.
19 P. Kumar, A. Deep and K.-H. Kim, Metal organic frameworks for sensing applications, *TrAC, Trends Anal. Chem.*, 2015, **73**, 39–53.
20 R. Kaur, K.-H. Kim, A. Paul and A. Deep, Recent advances in the photovoltaic applications of coordination polymers and metal organic frameworks, *J. Mater. Chem. A*, 2016, **4**, 3991–4002.
21 J. Mehta, N. Bhardwaj, S. K. Bhardwaj, K.-H. Kim and A. Deep, Recent advances in enzyme immobilization techniques: Metal-organic frameworks as novel substrates, *Coord. Chem. Rev.*, 2016, **322**, 30–40.

22 A. U. Czaja, N. Trukhan and U. Müller, Industrial applications of metal–organic frameworks, *Chem. Soc. Rev.*, 2009, **38**, 1284–1293.
23 H. Furukawa, K. E. Cordova, M. O'Keeffe and O. M. Yaghi, The chemistry and applications of metal-organic frameworks, *Science*, 2013, **341**, 1230444.
24 S. K. Bhardwaj, A. L. Sharma, N. Bhardwaj, M. Kukkar, A. A. Gill, K.-H. Kim and A. Deep, TCNQ-doped Cu-metal organic framework as a novel conductometric immunosensing platform for the quantification of prostate cancer antigen, *Sens. Actuators, B*, 2017, **240**, 10–17.
25 D. Cunha, M. Ben Yahia, S. Hall, S. R. Miller, H. Chevreau, E. Elkaïm, G. Maurin, P. Horcajada and C. Serre, Rationale of drug encapsulation and release from biocompatible porous metal–organic frameworks, *Chem. Mater.*, 2013, **25**, 2767–2776.
26 P. Horcajada, T. Chalati, C. Serre, B. Gillet, C. Sebrie, T. Baati, J. F. Eubank, D. Heurtaux, P. Clayette and C. Kreuz, Porous metal-organic-framework nanoscale carriers as a potential platform for drug delivery and imaging, *Nat. Mater.*, 2010, **9**, 172–178.
27 P. Horcajada, R. Gref, T. Baati, P. K. Allan, G. Maurin, P. Couvreur, G. Férey, R. E. Morris and C. Serre, Metal–organic frameworks in biomedicine, *Chem. Rev.*, 2011, **112**, 1232–1268.
28 S. Keskin and S. Kızılel, Biomedical applications of metal organic frameworks, *Ind. Eng. Chem. Res.*, 2011, **50**, 1799–1812.
29 V. Lykourinou, Y. Chen, X.-S. Wang, L. Meng, T. Hoang, L.-J. Ming, R. L. Musselman and S. Ma, Immobilization of MP-11 into a mesoporous metal–organic framework, MP-11@ mesoMOF: a new platform for enzymatic catalysis, *J. Am. Chem. Soc.*, 2011, **133**, 10382–10385.
30 A. C. McKinlay, R. E. Morris, P. Horcajada, G. Férey, R. Gref, P. Couvreur and C. Serre, BioMOFs: metal–organic frameworks for biological and medical applications, *Angew. Chem., Int. Ed.*, 2010, **49**, 6260–6266.
31 M. X. Wu and Y. W. Yang, Metal–Organic Framework (MOF)-Based Drug/Cargo Delivery and Cancer Therapy, *Adv. Mater.*, 2017, 1606134.
32 R. E. Morris, in *Antimicrobial Coatings and Modifications on Medical Devices*, Springer, 2017, p. 171.
33 J. Quirós, K. Boltes, S. Aguado, R. G. de Villoria, J. J. Vilatela and R. Rosal, Antimicrobial metal–organic frameworks incorporated into electrospun fibers, *Chem. Eng. J.*, 2015, **262**, 189–197.
34 A. C. McKinlay, P. K. Allan, C. L. Renouf, M. J. Duncan, P. S. Wheatley, S. J. Warrender, D. Dawson, S. E. Ashbrook, B. Gil and B. Marszalek, Multirate delivery of multiple therapeutic agents from metal-organic frameworks, *APL Mater.*, 2014, **2**, 124108.
35 R. E. Morris, Anti-microbial metal organic framework, US 2013/0171228A1, 2013.
36 C. E. Santo, D. Quaranta and G. Grass, Antimicrobial metallic copper surfaces kill Staphylococcus haemolyticus via membrane damage, *Microbiologyopen*, 2012, **1**, 46–52.
37 A. Casey, D. Adams, T. Karpanen, P. Lambert, B. Cookson, P. Nightingale, L. Miruszenko, R. Shillam, P. Christian and T. Elliott, Role of copper in reducing hospital environment contamination, *J. Hosp. Infect.*, 2010, **74**, 72–77.
38 S. R. Miller, E. Alvarez, L. Fradcourt, T. Devic, S. Wuttke, P. S. Wheatley, N. Steunou, C. Bonhomme, C. Gervais and D. Laurencin, A rare example of a porous Ca-MOF for the controlled release of biologically active NO, *Chem. Commun.*, 2013, **49**, 7773–7775.
39 M. Berchel, T. Le Gall, C. Denis, S. Le Hir, F. Quentel, C. Elléouet, T. Montier, J.-M. Rueff, J.-Y. Salaün and J.-P. Haelters, A silver-based metal–organic framework material as a 'reservoir'of bactericidal metal ions, *New J. Chem.*, 2011, **35**, 1000–1003.
40 Y. Liu, X. Xu, Q. Xia, G. Yuan, Q. He and Y. Cui, Multiple topological isomerism of three-connected networks in silver-based metal–organoboron frameworks, *Chem. Commun.*, 2010, **46**, 2608–2610.
41 H. S. Rodríguez, J. P. Hinestroza, C. Ochoa-Puentes, C. A. Sierra and C. Y. Soto, Antibacterial activity against *Escherichia coli* of Cu-BTC (MOF-199) metal organic framework immobilized onto cellulosic fibers, *J. Appl. Polym. Sci.*, 2014, **131**, 408–415.
42 A. R. Abbasi, K. Akhbari and A. Morsali, Dense coating of surface mounted CuBTC metal–organic framework nanostructures on silk fibers, prepared by layer-by-layer method under ultrasound irradiation with antibacterial activity, *Ultrason. Sonochem.*, 2012, **19**, 846–852.
43 S. Aguado, J. Quirós, J. Canivet, D. Farrusseng, K. Boltes and R. Rosal, Antimicrobial activity of cobalt imidazolate metal–organic frameworks, *Chemosphere*, 2014, **113**, 188–192.
44 A. Alonso, X. Munoz-Berbel, N. Vigués, J. Macanás, M. Munoz, J. Mas and D. N. Muraviev, Characterization of fibrous polymer silver/cobalt nanocomposite with enhanced bactericide activity, *Langmuir*, 2011, **28**, 783–790.
45 L. M. Plum, L. Rink and H. Haase, The essential toxin: impact of zinc on human health, *Int. J. Environ. Res. Public Health*, 2010, **7**, 1342–1365.
46 J. R. Schwartz, R. G. Marsh and Z. D. Draelos, Zinc and skin health: overview of physiology and pharmacology, *Dermatol. Surg.*, 2005, **31**, 837–847.
47 S. Pavlica, F. Gaunitz and R. Gebhardt, Comparative in vitro toxicity of seven zinc-salts towards neuronal PC12 cells, *Toxicol. in Vitro*, 2009, **23**, 653–659.
48 C. T. Ng, L. Q. Yong, M. P. Hande, C. N. Ong, L. E. Yu, B. H. Bay and G. H. Baeg, Zinc oxide nanoparticles exhibit cytotoxicity and genotoxicity through oxidative stress responses in human lung fibroblasts and Drosophila melanogaster, *Int. J. Nanomed.*, 2017, **12**, 1621.
49 S.-T. Yang, J.-H. Liu, J. Wang, Y. Yuan, A. Cao, H. Wang, Y. Liu and Y. Zhao, Cytotoxicity of zinc oxide nanoparticles: importance of microenvironment, *J. Nanosci. Nanotechnol.*, 2010, **10**, 8638–8645.
50 A. Punnoose, K. Dodge, J. W. Rasmussen, J. Chess, D. Wingett and C. Anders, Cytotoxicity of ZnO nano-

particles can be tailored by modifying their surface structure: a green chemistry approach for safer nanomaterials, *ACS Sustainable Chem. Eng.*, 2014, **2**, 1666–1673.

51 C. Tamames-Tabar, D. Cunha, E. Imbuluzqueta, F. Ragon, C. Serre, M. J. Blanco-Prieto and P. Horcajada, Cytotoxicity of nanoscaled metal–organic frameworks, *J. Mater. Chem. B*, 2014, **2**, 262–271.

52 F. Ren, B. Yang, J. Cai, Y. Jiang, J. Xu and S. Wang, Toxic effect of zinc nanoscale metal-organic frameworks on rat pheochromocytoma (PC12) cells in vitro, *J. Hazard. Mater.*, 2014, **271**, 283–291.

53 S. Beg, M. Rahman, A. Jain, S. Saini, P. Midoux, C. Pichon, F. J. Ahmad and S. Akhter, Nanoporous metal organic frameworks as hybrid polymer–metal composites for drug delivery and biomedical applications, *Drug Discovery Today*, 2017, **22**, 625–637.

54 C. Tamames-Tabar, E. Imbuluzqueta, N. Guillou, C. Serre, S. Miller, E. Elkaïm, P. Horcajada and M. Blanco-Prieto, A Zn azelate MOF: combining antibacterial effect, *CrystEngComm*, 2015, **17**, 456–462.

55 N. Bhardwaj, S. K. Bhardwaj, J. Mehta, M. K. Nayak and A. Deep, Bacteriophage conjugated IRMOF-3 as a novel opto-sensor for S. arlettae, *New J. Chem.*, 2016, **40**, 8068–8073.

56 M. Müller, S. Turner, O. I. Lebedev, Y. Wang, G. van Tendeloo and R. A. Fischer, Au@ MOF-5 and Au/MOx@ MOF-5 (M=Zn, Ti; x=1, 2): Preparation and Microstructural Characterisation, *Eur. J. Inorg. Chem.*, 2011, **2011**, 1876–1887.

57 L.-G. Qiu, Z.-Q. Li, Y. Wu, W. Wang, T. Xu and X. Jiang, Facile synthesis of nanocrystals of a microporous metal–organic framework by an ultrasonic method and selective sensing of organoamines, *Chem. Commun.*, 2008, 3642–3644.

58 M. Pfaller, D. Diekema, J. Rex, A. Espinel-Ingroff, E. Johnson, D. Andes, V. Chaturvedi, M. Ghannoum, F. Odds and M. Rinaldi, Correlation of MIC with outcome for Candida species tested against voriconazole: analysis and proposal for interpretive breakpoints, *J. Clin. Microbiol.*, 2006, **44**, 819–826.

59 G. B. Elion, S. Singer and G. H. Hitchings, Antagonists of nucleic acid derivatives VIII. Synergism in combinations of biochemically related antimetabolites, *J. Biol. Chem.*, 1954, **208**, 477–488.

60 J. Gutierrez, C. Barry-Ryan and P. Bourke, Antimicrobial activity of plant essential oils using food model media: efficacy, synergistic potential and interactions with food components, *Food Microbiol.*, 2009, **26**, 142–150.

61 G. Fotakis and J. A. Timbrell, In vitro cytotoxicity assays: comparison of LDH, neutral red, MTT and protein assay in hepatoma cell lines following exposure to cadmium chloride, *Toxicol. Lett.*, 2006, **160**, 171–177.

62 D. Gerlier and N. Thomasset, Use of MTT colorimetric assay to measure cell activation, *J. Immunol. Methods*, 1986, **94**, 57–63.

63 H. Liang, C. Jin, Y. Tang, F. Wang, C. Ma and Y. Yang, Cytotoxicity of silica nanoparticles on HaCaT cells, *J. Appl. Toxicol.*, 2014, **34**, 367–372.

64 J. G. Nguyen, K. K. Tanabe and S. M. Cohen, Postsynthetic diazeniumdiolate formation and NO release from MOFs, *CrystEngComm*, 2010, **12**, 2335–2338.

65 A. R. Chowdhuri, D. Bhattacharya and S. K. Sahu, Magnetic nanoscale metal organic frameworks for potential targeted anticancer drug delivery, imaging and as an MRI contrast agent, *Dalton Trans.*, 2016, **45**, 2963–2973.

66 T. Van Vu, H. Kosslick, A. Schulz, J. Harloff, E. Paetzold, J. Radnik, U. Kragl, G. Fulda, C. Janiak and N. D. Tuyen, Hydroformylation of olefins over rhodium supported metal-organic framework catalysts of different structure, *Microporous Mesoporous Mater.*, 2013, **177**, 135–142.

67 M. G. Bramucci, C. M. McCutchen, V. Nagarajan and S. M. Thomas, Microbial production of terephthalic acid and isophthalic acid, US 6187569B1, 2001.

68 L. Wang, B. Xiao, G. Wang and J. Wu, Synthesis of polycarbonate diol catalyzed by metal-organic framework Zn 4 O [CO 2-C 6 H 4-CO 2] 3, *Sci. China: Chem.*, 2011, **54**, 1468–1473.

69 G. Mahalakshmi and V. Balachandran, FT-IR and FT-Raman spectra, normal coordinate analysis and ab initio computations of Trimesic acid, *Spectrochim. Acta, Part A*, 2014, **124**, 535–547.

70 O. Yaghi, H. Li and T. Groy, Construction of porous solids from hydrogen-bonded metal complexes of 1, 3, 5-benzenetricarboxylic acid, *J. Am. Chem. Soc.*, 1996, **118**, 9096–9101.

71 Y.-X. Zhou, S.-G. Liang, J.-L. Song, T.-B. Wu, S.-Q. Hu, H.-Z. Liu, T. Jiang and B.-X. Han, Synthesis of Asymmetrical Organic Carbonates Catalyzed by Metal Organic Frameworks, *Acta Phys.-Chim. Sin.*, 2010, **26**, 939–945.

72 A. Aijaz, A. Karkamkar, Y. J. Choi, N. Tsumori, E. Rönnebro, T. Autrey, H. Shioyama and Q. Xu, Immobilizing highly catalytically active Pt nanoparticles inside the pores of metal–organic framework: a double solvents approach, *J. Am. Chem. Soc.*, 2012, **134**, 13926–13929.

73 X. Kang, Q. Zhu, X. Sun, J. Hu, J. Zhang, Z. Liu and B. Han, Highly efficient electrochemical reduction of CO 2 to CH 4 in an ionic liquid using a metal–organic framework cathode, *Chem. Sci.*, 2016, **7**, 266–273.

74 M. Meilikhov, K. Yusenko, D. Esken, S. Turner, G. Van Tendeloo and R. A. Fischer, Metals@ MOFs–loading MOFs with metal nanoparticles for hybrid functions, *Eur. J. Inorg. Chem.*, 2010, **2010**, 3701–3714.

75 S. Lin, X. Liu, L. Tan, Z. Cui, X. Yang, K. W. Yeung, H. Pan and S. Wu, Porous Iron-Carboxylate Metal–Organic Framework: A Novel Bioplatform with Sustained Antibacterial Efficacy and Nontoxicity, *ACS Appl. Mater. Interfaces*, 2017, **9**, 19248–19257.

76 M. Bajaj, S. K. Pandey, T. Nain, S. K. Brar, P. Singh, S. Singh, N. Wangoo and R. K. Sharma, Stabilized cationic dipeptide capped gold/silver nanohybrids: Towards enhanced antibacterial and antifungal efficacy, *Colloids Surf., B*, 2017, **158**, 397.

77 S. Gurunathan, J. W. Han, D.-N. Kwon and J.-H. Kim, Enhanced antibacterial and anti-biofilm activities of silver nanoparticles against Gram-negative and Gram-positive bacteria, *Nanoscale Res. Lett.*, 2014, **9**, 373.
78 E. B. Hirsch and V. H. Tam, Detection and treatment options for Klebsiella pneumoniae carbapenemases (KPCs): an emerging cause of multidrug-resistant infection, *J. Antimicrob. Chemother.*, 2010, **65**, 1119–1125.
79 Z. A. Qureshi, D. L. Paterson, B. A. Potoski, M. C. Kilayko, G. Sandovsky, E. Sordillo, B. Polsky, J. M. Adams-Haduch and Y. Doi, Treatment outcome of bacteremia due to KPC-producing Klebsiella pneumoniae: superiority of combination antimicrobial regimens, *Antimicrob. Agents Chemother.*, 2012, **56**, 2108–2113.
80 O. Zarkotou, S. Pournaras, P. Tselioti, V. Dragoumanos, V. Pitiriga, K. Ranellou, A. Prekates, K. Themeli-Digalaki and A. Tsakris, Predictors of mortality in patients with bloodstream infections caused by KPC-producing Klebsiella pneumoniae and impact of appropriate antimicrobial treatment, *Clin. Microbiol. Infect.*, 2011, **17**, 1798–1803.